

Cellular Variability of RpoS Expression Underlies Subpopulation Activation of an Integrative and Conjugative Element

Ryo Miyazaki¹, Marco Minoia¹, Nicolas Pradervand, Sandra Sulser, Friedrich Reinhard, Jan Roelof van der Meer*

Department of Fundamental Microbiology, University of Lausanne, Lausanne, Switzerland

Abstract

Conjugative transfer of the integrative and conjugative element ICE_{clc} in the bacterium *Pseudomonas knackmussii* is the consequence of a bistable decision taken in some 3% of cells in a population during stationary phase. Here we study the possible control exerted by the stationary phase sigma factor RpoS on the bistability decision. The gene for RpoS in *P. knackmussii* B13 was characterized, and a loss-of-function mutant was produced and complemented. We found that, in absence of RpoS, ICE_{clc} transfer rates and activation of two key ICE_{clc} promoters (P_{int} and P_{inR}) decrease significantly in cells during stationary phase. Microarray and gene reporter analysis indicated that the most direct effect of RpoS is on P_{inR} , whereas one of the gene products from the P_{inR} -controlled operon (InrR) transmits activation to P_{int} and other ICE_{clc} core genes. Addition of a second *rpoS* copy under control of its native promoter resulted in an increase of the proportion of cells expressing the P_{int} and P_{inR} promoters to 18%. Strains in which *rpoS* was replaced by an *rpoS-mCherry* fusion showed high mCherry fluorescence of individual cells that had activated P_{int} and P_{inR} , whereas a double-copy *rpoS-mCherry*-containing strain displayed twice as much mCherry fluorescence. This suggested that high RpoS levels are a prerequisite for an individual cell to activate P_{inR} and thus ICE_{clc} transfer. Double promoter-reporter fusions confirmed that expression of P_{inR} is dominated by extrinsic noise, such as being the result of cellular variability in RpoS. In contrast, expression from P_{int} is dominated by intrinsic noise, indicating it is specific to the ICE_{clc} transmission cascade. Our results demonstrate how stochastic noise levels of global transcription factors can be transduced to a precise signaling cascade in a subpopulation of cells leading to ICE activation.

Citation: Miyazaki R, Minoia M, Pradervand N, Sulser S, Reinhard F, et al. (2012) Cellular Variability of RpoS Expression Underlies Subpopulation Activation of an Integrative and Conjugative Element. *PLoS Genet* 8(7): e1002818. doi:10.1371/journal.pgen.1002818

Editor: Diarmaid Hughes, Uppsala University, Sweden

Received: February 5, 2012; **Accepted:** May 23, 2012; **Published:** July 12, 2012

Copyright: © 2012 Miyazaki et al. This is an open-access article distributed under the terms of the Creative Commons Attribution License, which permits unrestricted use, distribution, and reproduction in any medium, provided the original author and source are credited.

Funding: This work was supported by grants from the Swiss National Science Foundation (31003A_124711 and 3100A0-108199). The funders had no role in study design, data collection and analysis, decision to publish, or preparation of the manuscript.

Competing Interests: The authors have declared that no competing interests exist.

* E-mail: janroelof.vandermeer@unil.ch

† These authors contributed equally to this work.

Introduction

Integrative and conjugative elements (ICE) are a newly recognized class of mobile DNA elements in prokaryotes [1–4]. ICE come in different families, represented by the host cell range and gene similarities, but all have a similar mechanistic ‘life-style’ [2]. Under most circumstances the ICE resides in one or more positions in the host chromosome like a prophage [5]. At frequencies of typically less than 10^{-2} per cell and under particular growth conditions or environmental signals ICE excise by recombination between short direct repeats at either end (within the attachment sites *attL* and *attR*) [6–8]. The double-stranded excised ICE can undergo DNA processing as for plasmid conjugation [9], and transfers a single-stranded ICE-DNA to a new host cell. In the new host cell the ICE-DNA is replicated and integrates by site-specific recombination between the ICE-located *attP*-site and the chromosomal attachment site *attB* [1,2]. Interestingly, many ICE integrate in genes for tRNA [10] and ICE integrase sequences suggest phage ancestry [11].

ICE have attracted broad interest because, similar to plasmids, they can carry a large number of auxiliary genes in addition to the genes necessary for their basic functioning, which can provide selective advantages to the host cell. For example, several ICE carry genes for antibiotic resistance [12–14], for iron scavenging [15,16], for diguanylate cyclases that can enhance host survival [17], for plant symbiosis [18] or for metabolism of chloro- and aminoaromatic compounds [19–21]. Although some ICE have been detected by their self-transferability, a large number of ICE-related elements with unknown mobility has been discovered through genome comparisons [22–24]. Some of those may be mobilized with help of other elements [25], but others may represent elements in retrograde evolution that once were capable of initiating conjugation, but which are now rendered immobile [23]. In more general terms one therefore often speaks of ‘genomic islands’ [1] or ‘regions of genomic plasticity’ [24], which include both ICE and ICE-like elements. Genome comparisons among closely related strains have suggested that a significant fraction (perhaps as much as 20%) of strain-to-strain variation may be due

Author Summary

Horizontal gene transfer is one of the amazing phenomena in the prokaryotic world, by which DNA can be moved between species with means of a variety of specialized “elements” and/or specific host cell mechanisms. In particular the molecular decisions that have to be made in order to transfer DNA from one cell to another are fascinating, but very little is known about this at a cellular basis. Here we study a member of a widely distributed type of mobile DNA called “integrative and conjugative elements” or ICE. ICE*clc* normally resides in the chromosome of its bacterial host, but can excise from the chromosome and prepare for conjugation. Interestingly, the decision to excise ICE*clc* is made in only 3%–5% of cells in a clonal population in stationary phase. We focus specifically on the question of which mechanism may be responsible for setting this threshold level of ICE*clc* activation. We find that ICE*clc* activation is dependent on the individual cell level of the stationary phase sigma factor RpoS. The noise in RpoS expression across a population of cells thus sets the “threshold” for ICE*clc* to excise and prepare transfer.

to the presence of different types of genomic islands [24,26,27]. Such comparisons have further implied that genomic islands are largely responsible for the adaptive capacities of prokaryotic species [28].

Although several ICE have been genetically and functionally characterized, and their general importance for bacterial evolution and adaptation is now widely appreciated, still very little is known about their cell biology [2]. One of the most intriguing aspects of the functioning of an ICE is its low frequency of conjugation (e.g., 1% or less of a population of cells), which suggests that in only very few individual cells in a clonal population a decision is made to activate the ICE. The types of mechanisms and regulatory control that can achieve such low frequency differentiation are still widely unexplored. Some ICE bear regulatory systems controlling excision that involve phage-type repressors [29–31], which therefore may behave similar as the phage lambda bistable lysogenic/lytic switch [32]. Other ICE-classes, however, bear no gene functions with significant homologies to known phage lytic switches. Previously, we showed that excision and transfer of the element ICE*clc* in *Pseudomonas knackmussii* B13 must be the consequence of a bistable switch that culminates in the activation of the *intB13* integrase promoter (hereafter named P_{int}) in 3% of cells during stationary phase [33]. ICE*clc* is a 103-kb sized element with strong homologies to a large number of genomic islands in *Beta*- and *Gamma*proteobacteria, and is named after its propensity to provide the host cell with the capacity to metabolize chlorinated catechols, encoded by the *clc* genes [21]. Two identical ICE*clc* copies reside in the chromosome of strain B13, which are interspaced by 340 kb (Miyazaki, unpublished). Activation of the *intB13* integrase leads to excision and formation of a closed circular ICE*clc* intermediate [33]. Transfer of the circular intermediate is dependent on a DNA relaxase, which makes a single-stranded break, but, exceptionally, can initiate transfer at two origins of transfer (*oriT*) on ICE*clc* [9]. Single cell studies using fluorescent reporter fusions showed that P_{int} activation was preceded by and dependent on expression of a protein named InrR (for INtegrase RRegulator) in the same individual cell (Figure 1). InrR is encoded in a small four-gene operon on ICE*clc* under control of another bistably expressed promoter (P_{inR}) [33]. This suggested that ICE excision and activation in general may be

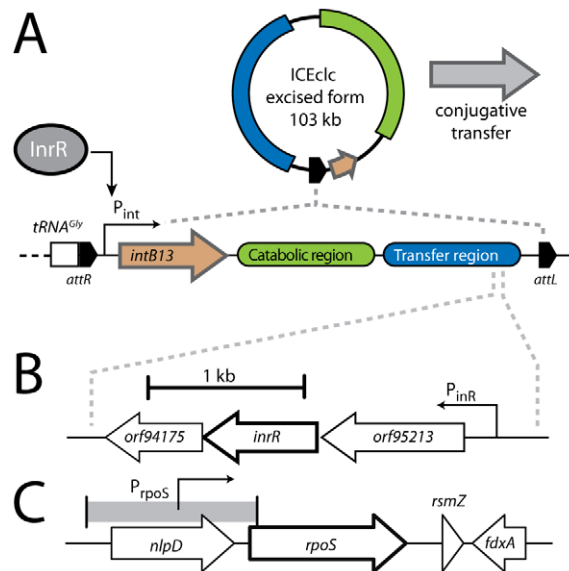


Figure 1. Schematic representation of the ICE*clc* genetic layout and relevant regulatory features. (A) Excised and integrated ICE*clc* (not to scale) with its flanking *attL* and *attR* sites, and the 18-bp repeat sequences (black pentangle) that are the target of the *IntB13* integrase. The ‘transfer region’ denotes the ~50 kb ICE*clc* part largely conserved with other genomic islands [21]. (B) The region of the open reading frames under control of P_{inR} , among which *inrR*, the product of which has been implicated in relaying bistable expression to the P_{int} promoter [34]. (C) The gene region around *rpoS* in strain B13. doi:10.1371/journal.pgen.1002818.g001

the consequence of a bistable switch, and that the frequency of ON-setting is a determining factor for the frequency of ICE conjugation. Bistability as a phenomenon is most well-known from competence development and sporulation in *Bacillus subtilis*, which lead to phenotypically differentiated cells [32,34,35]. Although bistability is thought to originate from stochastic expression noise, this in itself is not sufficient to ‘lock’ cells in different phenotypic behaviour, but rather needs to be amplified and stabilized by regulatory mechanisms that include double positive feedback loops or double negative loops [32]. On the other hand, it is conceivable that the noisiness sets the threshold for the proportion of cells that display the bistable trait.

The goal of the underlying work was to explore whether noisiness may lay at the basis of determining the proportion of cells in which ICE*clc* becomes active. We focused our attention on both P_{int} and P_{inR} promoters, which are expressed during stationary phase and only in a subpopulation of cells [8,33,36]. Initiation of ICE*clc* transfer in stationary phase cells further suggested involvement of a specific sigma factor such as RpoS (σ^s). RpoS is the stress-starvation sigma factor that in *P. aeruginosa* controls the expression of some 772 genes at the onset of stationary phase [37], 40% of which have also been identified as quorum-sensing controlled. Deletion of *rpoS* in *P. aeruginosa* does not result in a dramatically changed phenotype, although such mutants survive 50-fold less well to heat and salt shocks than wild-type, and produce less extracellular proteins such as elastase, exotoxin A, and alginate [38]. In order to establish the role of a stationary phase sigma factor in activation of ICE*clc*, we identified an *rpoS*-gene in *P. knackmussii* B13 and studied the effects of interruption and subsequent complementation using single-cell reporter gene fusions to P_{int} and P_{inR} . Interestingly, a B13 wild-type equipped with a second *rpoS* gene copy displayed a much higher

subpopulation of cells expressing both P_{int} and P_{inR} promoters. To study whether actually individual cell levels of RpoS could be somehow deterministic for the activation of ICE clc we replaced native *rpoS* by a gene for an active RpoS-mCherry fusion protein. Finally, we measured contributions of intrinsic and extrinsic noise on P_{int} and P_{inR} promoters from covariance in the expression of double gene reporters placed in single copy on different parts of the B13 chromosome [39]. Our results indicate that individual cells with the highest RpoS levels in the population are more prone to activate P_{int} and P_{inR} , which suggests that the stochastic variation in RpoS levels across a population of cells is transduced into ICE clc activation and transfer in a small subpopulation.

Results

Identification of the *rpoS* gene from *P. knackmussii* strain B13

In order to identify the *rpoS* gene of *P. knackmussii* strain B13 we used PCR amplification with primers designed against conserved regions in a multiple alignment of *rpoS* sequences of *P. aeruginosa*, *P. putida* KT2440 and *P. fluorescens* (Figure S1). The nucleotide sequence of the amplified fragment from strain B13 showed high homology to a set of *rpoS* genes from other pseudomonads, with a percentage nucleotide identity between $rpoS_{B13}$ and *rpoS* from different *P. aeruginosa* strains of 83% over 989 bp. The predicted amino acid sequence of RpoS $_{B13}$ positioned most closely to that of *P. aeruginosa* PAO1 (Figure S2). Flanking regions of $rpoS_{B13}$ were subsequently recovered from a draft genome sequence of *P. knackmussii* B13 (Miyazaki, unpublished data), which showed that the *rpoS* region of strain B13 is syntenic to that in *P. aeruginosa* PAO1 with a gene for a lipoprotein (*nlpD*) upstream of *rpoS*, and an *rsmZ*-like gene and a gene for a ferredoxin (*fdxA*) downstream (Figure 1). We therefore concluded that this region in B13 most likely encodes a similar stationary phase sigma factor as in *P. aeruginosa*.

A single crossover *rpoS* mutant was produced by marker insertion (strain B13-2671, Figure S3, Table 1). Despite repeated attempts we were not successful in producing a double recombinant with an internal *rpoS* deletion. However, it was possible to replace $rpoS_{B13}$ by a gene for a RpoS $_{B13}$ -mCherry fusion protein (see below). Maximum specific growth rates of strain B13-2671 (*rpoS*) on MM with 5 mM 3CBA were similar as B13 wild-type (0.22 ± 0.01 versus 0.26 ± 0.01 h $^{-1}$, respectively), but the onset of exponential growth was slightly delayed in B13-2671 (*rpoS*) (Figure S4A). Reversion to the wild-type allele occurred in less than 1% of cells in stationary phase (Figure S4B).

RpoS is implicated in expression of the bistable ICE clc promoters P_{inR} and P_{int}

The fact that most of the core genes of ICE clc are solely expressed in stationary phase *P. knackmussii* B13 cells [36], and the presence of sequence features typical for RpoS in the P_{inR} promoter [33] had suggested an implication of RpoS in controlling ICE clc stationary phase expression. Inactivation of *rpoS* in B13 indeed resulted in reduced expression of both P_{inR} and P_{int} promoters. This was evident, first of all, from a reduced proportion of cells in a B13-2673 (*rpoS*) compared to B13 wild-type population expressing eCherry and eGFP above detection threshold from single copy transcriptional fusions to P_{inR} and P_{int} respectively (Figure 2B, Table 2). Secondly, stationary phase cells of B13-2673 (*rpoS*) produced a lower average reporter fluorescence signal than wild-type cells (Table 2). In most individual cells the magnitudes of eGFP and eCherry expression correlated, confirming that P_{inR} and

P_{int} were expressed in the same cell (Figure 2B). Both eCherry and eGFP were not visibly expressed in B13-2673 (*rpoS*) cells examined after 24 h in stationary phase, but after 72 h a small fraction of cells still developed eGFP and eCherry fluorescence (Figure 2B). This delay (48 h) is much longer than would be expected from the slight growth delay (5 h) of B13-2673 (*rpoS*) compared to B13-78 wild-type to reach stationary phase (Figure S4). Late (72 h) expression of P_{int} and P_{inR} in B13-2673 (*rpoS*) was not due to reversion of the *rpoS* mutation (Figure S4B).

To confirm that the effect on P_{int} and P_{inR} expression was caused by a disruption of *rpoS*, we complemented strain B13-2673 with a single copy mini-Tn5 insertion containing $rpoS_{B13}$ under control of its own promoter (P_{rpoS} , Figure 2A). Both the proportion of cells and their average fluorescence levels of both fluorescent markers from P_{inR} and P_{int} were restored to wild-type levels in the *rpoS*-complemented strain *P. knackmussii* B13-2993 (Figure 2B, Table 2). The number of cells expressing autofluorescent proteins from both promoters was even slightly higher in the *rpoS* complemented strain than in B13 wild-type after 96 h in stationary phase, although this was not a statistically significant difference (Table 2).

We can thus conclude from this part that, because both the expression level of eGFP and eCherry in single cells and also the percentage of cells that expressed both markers in strain B13-2673 (*rpoS*) was significantly lower than in B13 wild-type and the *rpoS*-complemented strain (B13-2993), RpoS is necessary for achieving native transcription levels from the P_{inR} promoter (i.e., within 48 h of stationary phase). On the other hand, RpoS is not absolutely essential, since cells with interrupted *rpoS* gene eventually (96 h) express P_{inR} and P_{int} , which was not due to reversion of the *rpoS* mutation (Figure S4B).

Direct influence of RpoS on integrase expression

Since the observed lower expression from the integrase promoter (P_{int}) in the *rpoS* mutant could be the result of either less InrR being formed from P_{inR} , or of a direct control by RpoS of P_{int} , we compared eGFP expression from a single copy P_{int} -*egfp* transcriptional fusion in B13, the B13 *rpoS* mutant (B13-2976) and a B13 lacking both *inrR* copies (B13-2979, Table 1). Interestingly, the proportion of cells expressing eGFP and their average fluorescence were much lower in a strain lacking both *inrR* copies than in the strain missing RpoS (Figure S5, Table 3), suggesting that the major influence of RpoS is indirectly via InrR.

Since the proportion of cells expressing eGFP from P_{int} in an *inrR* $^{-/-}$ background was already so low, it was not possible to detect statistically significant differences to a strain that would carry the triple *rpoS* and *inrR* $^{-/-}$ mutations (Table 3). For this reason, we produced the triple *rpoS inrR* $^{-/-}$ mutation in a B13 strain containing a dual reporter of P_{int} -*egfp* and P_{inR} -*echerry* (B13-3091), and correlated eGFP to eCherry expression. Since this strain would be devoid of InrR-mediated expression of P_{int} , we expected that expression of *egfp* from P_{int} in absence of *rpoS* would be lower than expression of *echerry* from P_{inR} . Indeed, there was a slight tendency for the mean proportion of cells expressing eGFP (from P_{int}) in strain B13-3091 (*rpoS, inrR* $^{-/-}$) to be lower than that expressing eCherry (from P_{inR}), although this was only poorly significant after 96 h ($P = 0.04$), again because of the very low subpopulation sizes (<0.5%, Table 2). Purified and reconstituted RpoS-RNA polymerase from *E. coli* bound DNA fragments encompassing P_{int} in *in vitro* electrophoretic mobility shift assays (K. Globig and J. van der Meer, unpublished data). This suggests that transcription from P_{int} is both indirectly (via InrR) and directly dependent on RpoS.

Table 1. Strains used in this study.

Strain number	Description	Remarks	Reference
78	<i>Pseudomonas knackmussii</i> B13	Original host for ICE clc	[49]
1292	<i>Pseudomonas putida</i> UWC1, Rif ^R		[61]
1346	<i>P. knackmussii</i> B13 mini-Tn5(P _{int,jim2} - <i>egfp</i> , Km ^R)	<i>jim2 intB13</i> - promoter fragment in 78	[58]
2201	<i>P. knackmussii</i> B13 <i>inrR</i> ^{-/-}	Both copies of <i>inrR</i> deleted	[34]
2581	<i>P. knackmussii</i> B13 mini-Tn5(P _{int} - <i>egfp</i> , P _{inrR} - <i>echerry</i> , Km ^R)	Dual P _{int} P _{inrR} reporter strain from 78	[34]
2671	<i>P. knackmussii</i> B13 <i>rpoS</i> , Tet ^R	Single recombinant via integration of pME3087-' <i>rpoS</i> '	This study
2673	<i>P. knackmussii</i> B13 <i>rpoS</i> , mini-Tn5(P _{int} - <i>egfp</i> , P _{inrR} - <i>echerry</i> , Km ^R), Tet ^R	Dual P _{int} P _{inrR} reporter strain from 2671	This study
2717	<i>P. knackmussii</i> B13 mini-Tn5(P _{int} - <i>egfp</i> , Km ^R), mini-Tn5(P _{int} - <i>echerry</i> , Tet ^R)	Double P _{int} reporter in 78	This study
2976	<i>P. knackmussii</i> B13 <i>rpoS</i> , mini-Tn5(P _{int,jim2} - <i>egfp</i> , Km ^R)	P _{int} [jim2] reporter strain from 2671	This study
2979	<i>P. knackmussii</i> B13 <i>inrR</i> ^{-/-} , mini-Tn5(P _{int,jim2} - <i>egfp</i> , Km ^R)	P _{int} [jim2] reporter strain from 2201	This study
2993	<i>P. knackmussii</i> B13 <i>rpoS</i> , mini-Tn5(P _{rpoS} - <i>rpoS</i> , Km ^R), mini-Tn5(P _{int} - <i>egfp</i> , P _{inrR} - <i>echerry</i>), Tet ^R	<i>rpoS</i> complemented in 2673	This study
3091	<i>P. knackmussii</i> B13 <i>inrR</i> ^{-/-} , <i>rpoS</i> , mini-Tn5(P _{int} - <i>egfp</i> , P _{inrR} - <i>echerry</i> , Km ^R)	<i>rpoS</i> mutant in 2201 background, with dual P _{int} P _{inrR} reporter	This study
3165	<i>P. knackmussii</i> B13 mini-Tn5(P _{rpoS} - <i>mcherry</i> , Km ^R)	P _{rpoS} reporter strain from 78	This study
3183	<i>P. knackmussii</i> B13 mini-Tn5(P _{int} - <i>egfp</i>), mini-Tn5(P _{rpoS} - <i>mcherry</i> , Km ^R)	P _{int} reporter strain from 3165	This study
3189	<i>P. knackmussii</i> B13 mini-Tn5(P _{inrR} - <i>egfp</i>), mini-Tn5(P _{rpoS} - <i>mcherry</i> , Km ^R)	P _{inrR} reporter strain from 3165	This study
3195	<i>P. knackmussii</i> B13 mini-Tn5(P _{int} - <i>egfp</i>), mini-Tn5(P _{int} - <i>echerry</i> , Tet ^R), mini-Tn5(P _{inrR} - <i>orf95213-inrR</i> , Km ^R)	Extra copy of <i>inrR</i> in 2717	This study
3201	<i>P. knackmussii</i> B13 mini-Tn5(P _{int} - <i>egfp</i>), mini-Tn5(P _{int} - <i>echerry</i> , Tet ^R), mini-Tn5(P _{rpoS} - <i>rpoS</i> , Km ^R)	Extra copy of <i>rpoS</i> in 2717	This study
3228	<i>P. knackmussii</i> B13 <i>rpoS</i> , mini-Tn5(P _{rpoS} - <i>mcherry</i> , Km ^R), Tet ^R	Transcriptional P _{rpoS} reporter strain from 2671	This study
3257	<i>P. knackmussii</i> B13 mini-Tn5(P _{int} - <i>egfp</i> , P _{inrR} - <i>echerry</i>), mini-Tn5(P _{inrR} - <i>orf95213-inrR</i> , Km ^R)	Extra copy of <i>inrR</i> in 2581	This study
3260	<i>P. knackmussii</i> B13 mini-Tn5(P _{int} - <i>egfp</i> , P _{inrR} - <i>echerry</i>), mini-Tn5(P _{rpoS} - <i>rpoS</i> , Km ^R)	Extra copy of <i>rpoS</i> in 2581	This study
3555	<i>P. knackmussii</i> B13 <i>rpoS</i> - <i>mCherry</i> , mini-Tn5(P _{inrR} - <i>egfp</i>), Km ^R	<i>rpoS</i> replaced by <i>rpoS</i> - <i>mcherry</i> (translational fusion), plus single copy transcriptional P _{inrR} - <i>egfp</i> fusion	This study
3564	<i>P. knackmussii</i> B13 <i>rpoS</i> - <i>mcherry</i> , mini-Tn5(P _{int} - <i>egfp</i>), Km ^R	as 3555, with single copy transcriptional P _{int} - <i>egfp</i> fusion	This study
3641	<i>P. knackmussii</i> B13 mini-Tn5(P _{inrR} - <i>egfp</i> , Km ^R), mini-Tn5(P _{inrR} - <i>echerry</i> , Tet ^R)	Double P _{inrR} reporter in 78	This study
3712	<i>P. knackmussii</i> B13 <i>rpoS</i> - <i>mCherry</i> , mini-Tn5(P _{int} - <i>egfp</i>), mini-Tn5(P _{rpoS} - <i>rpoS</i> - <i>mcherry</i> , Km ^R)	Extra copy of <i>rpoS</i> - <i>mCherry</i> fusion in 3564	This study

doi:10.1371/journal.pgen.1002818.t001

ICE clc transfer and core gene expression is reduced in absence of functional RpoS

Whereas expression of the reporter gene fusions was interpreted as being representative for the behaviour of the native P_{int} and P_{inrR} promoters on ICE clc , we also determined ICE clc core gene expression and transfer frequencies from B13 wild-type or derivatives as donor and *P. putida* UWC1 as recipient. Expression of the ICE clc core genes in stationary phase cells measured by microarray analysis was lower (up to 27-fold) for both B13-2671 (*rpoS*) and B13-2201 (*inrR*^{-/-}) compared to B13 wild-type (Figure S6). Interestingly, expression of the *inrR* operon was not only downregulated in B13-2671 (*rpoS*) but also in B13-2201 (*inrR*^{-/-}) (Figure S6), suggesting autoregulation by InrR.

Not only ICE clc core gene expression but also transfer frequencies were significantly lower at all time points from B13-2673 (*rpoS*) or B13-3091 (*rpoS*, *inrR*^{-/-}) than from B13-2581 wild-type or the *rpoS*-complemented B13 *rpoS* mutant (B13-2993) as donor (Figure 3, Table S1). ICE clc transfer frequencies from the complemented B13 *rpoS* mutant were not significantly different than those from B13 wild-type. Transfer frequencies from B13-2673 (*rpoS*) as donor were significantly higher than from B13-3091

(*rpoS*, *inrR*^{-/-}) as donor, but only after 96 h mating time (Table S1). These results thus corroborated that RpoS is favorable (but not essential) for expression of ICE clc core genes and thus for conjugative transfer. RpoS exerts its control mainly via its interaction with the *inrR* promoter, with InrR relaying the activation further to other ICE clc core genes, but also via direct interaction at P_{int}.

Correlation between *rpoS* and P_{int} or P_{inrR} expression

Since in the absence of RpoS the proportion of cells expressing P_{int} or P_{inrR} in the population diminishes but not completely disappears, we wondered whether the levels of RpoS or the magnitude of *rpoS* expression in individual B13 cells are a precondition for cells to become locked in the P_{inrR} - P_{int} bistable 'ON'-state. Expression from P_{rpoS} is maximal at the end of the exponential phase and in stationary phase, as shown by the appearance of mCherry fluorescence from single copy P_{rpoS}-*mcherry* and *rpoS*-*mCherry* fusions in B13-3165 or B13-3564, respectively (Figure S7), which coincides with the timepoint of activation of P_{inrR} and P_{int}.

To correlate expression from *rpoS* with that of P_{int} or P_{inrR} in individual cells we created B13 derivatives with single copy

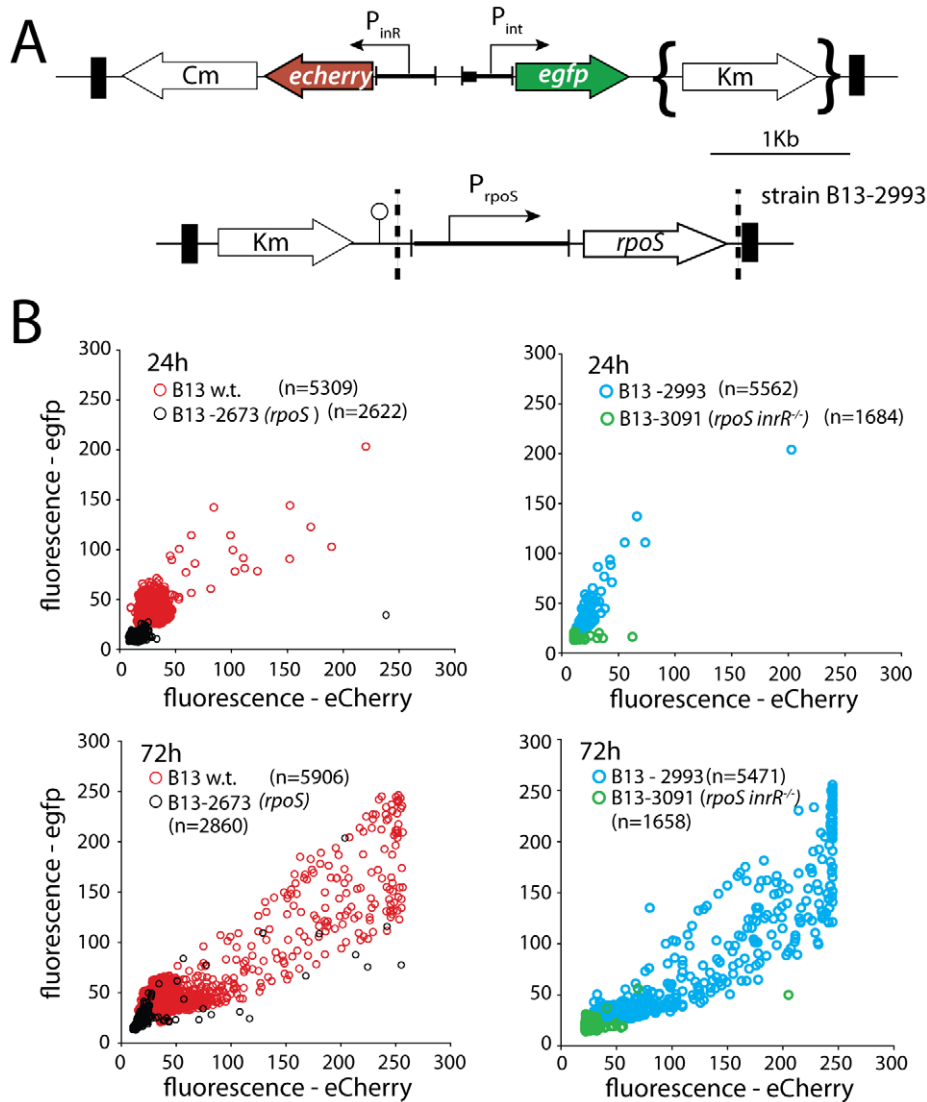


Figure 2. Effect of *rpoS* interruption on reporter gene expression from two key bistable promoters (P_{int} and P_{inR}) controlling ICE clc activity in stationary phase *P. knackmussii* cells grown on 3CBA. (A) Relevant details of the P_{int} -*egfp*, P_{inR} -*echerry* mini-transposon reporter construct and of the mini-transposon introducing the native *rpoS* gene under control of its own promoter (only in the complemented strain B13-2993, orientation of this insert unknown). Transposon boundaries indicated by thick black lines. (B) Scatter plots showing eGFP (from P_{int}) and eCherry (from P_{inR}) fluorescence intensities in single cells (circles) of B13-2581 (wild-type), B13-2673 (*rpoS*), B13-2993 (*rpoS* complemented in *trans* by mini-Tn with *rpoS*), or B13-3091 (*rpoS*, *inrR*^{-/-}) at 24 h and 72 h in stationary phase. Note the camera saturation in the eCherry channel above 256 units (8-bits). For signal quantification and significance testing, see Table 2. doi:10.1371/journal.pgen.1002818.g002

P_{rpoS} -*mcherry* and P_{int} -*egfp* or P_{inR} -*egfp* fusions (B13-3183 and B13-3189, respectively). mCherry expression from P_{rpoS} in stationary phase is normally distributed among all cells with a mean around 50 RFU (Figure 4A). In contrast, simultaneous eGFP expression from P_{int} -*egfp* or P_{inR} -*egfp* in B13-3183 and B13-3189, respectively, occurs highly skewed in only 3% of cells (Figure 4A). However, there was no particular correlation between expression of mCherry and eGFP in single cells.

To better account for post-transcriptional effects on RpoS expression we repeated the experiment with B13 derivatives expressing RpoS translationally fused to mCherry at its C-terminal end (RpoS-mCherry) from the original *rpoS* locus. This was done by substituting the native *rpoS*_{B13} by the *rpoS*_{B13}-*mcherry* allele. Similar as B13 wild-type RpoS also RpoS-mCherry was expressed

during stationary phase in all cells with normal distribution (Figure 4B), and eGFP was again expressed in 3–6% of cells in the population from either the P_{int} or P_{inR} promoter (strains B13-3564 and B13-3555, respectively). RpoS-mCherry but not an N-terminal mCherry-RpoS fusion protein complemented B13-*rpoS* for bistable P_{int} or P_{inR} -dependent eGFP expression (data not shown). This indicated that the RpoS-mCherry fusion protein functionally replaces B13 wild-type RpoS. Significantly, only B13-3564 and B13-3555 cells expressing the highest RpoS-mCherry levels had also activated eGFP from P_{int} or P_{inR} , respectively, although not all cells with high RpoS-mCherry levels expressed high levels of eGFP (Figure 4C). This suggests that the RpoS level *per se* is not sufficient to elicit P_{inR} or P_{int} expression but is a precondition for P_{inR} - or P_{int} -expression to occur.

Table 2. Effect of *rpoS* inactivation on reporter fluorescence from a single-copy P_{int} -*egfp*; P_{inR} -*eCherry* fusion in *P. knackmussii* strain B13 and derivatives.

Time (h) ¹	A) B13-2581 (Wild-type)			B) B13-2673 (<i>rpoS</i>)			C) B13-2993 (<i>rpoS</i> , mini-Tn5[<i>P_{rpoS}⁺rpoS</i>])			D) B13-3091 (<i>rpoS</i> , <i>inrR</i> ^{-/-})			
	eGFP ²	% ³	signif ⁴	eGFP	%	signif	eGFP	%	signif	eGFP	%	eCherry %	signif
24	89±8	0.7±0.2	AD	21±0.8	1.0±0.5		47±24	0.8±0.4		<10	<0.1		
48	135±3	3.0±0.7	AB, AD	86±40	0.9±0.4	BC	121±11	3.2±0.4	CD	<10	0.17±0.08	39±7	0.22±0.2 P=0.36 ⁵
72	150±6	2.8±0.1	AB, AD	65±10	0.8±0.2	BC	133±10	3.8±1.2	CD	19±32	0.23±0.40	57±24	0.2±0.04 P=0.44
96	116±13	1.9±0.2	AD	95±12	1.6±0.4	BC, BD	108±12	3.2±0.6	CD	42±36	0.25±0.21	70±18	0.6±0.02 P=0.04

¹Time after culture inoculation. Time 24 h is onset of stationary phase.

²Average eGFP or eCherry (in bold) fluorescence (relative units) within the subpopulation of cells across biological triplicates (see Figure S7 for explanation).

³Average subpopulation of cells (percent of total) expressing *egfp* from P_{int} (or *eCherry* from P_{inR} in bold) determined from cumulative distribution curves among biological triplicates.

⁴Significance of difference (P<0.05) in a Tukey's post-hoc test on sample variances of subpopulation sizes per time group across all strains (one-way ANOVA).

⁵Calculated P-values in pair-wise homoscedastic T-test between proportions of eGFP and eCherry expressing cells.

doi:10.1371/journal.pgen.1002818.t002

Globally increasing RpoS levels augments the subpopulation size of cells expressing the P_{inR} promoter

To artificially increase RpoS expression more globally across all cells in the population, with the idea that this would precondition more cells to activate P_{inR} and P_{inb} , an additional *rpoS*_{B13} copy under control of its own promoter was introduced by mini-Tn5 transposition (B13-3260, Figure 5A). Strikingly, ~18% of all cells in stationary phase cultures of B13-3260 (*rpoS*⁺) expressed eGFP from P_{int} and eCherry from P_{inR} compared to 5% in B13-2581 wild-type (Figure 5B–5E). ICE_{cl} transfer from B13-3260 (*rpoS*⁺) as donor to *P. putida* UWC1 as recipient was twice as high as with B13 wild-type after the same mating contact time, although this was not a statistically significant difference (48 h, Table S2). In contrast, B13 with an extra copy of *inrR* (strain B13-3257) did not significantly differentially express both reporter genes from P_{inR} and P_{int} (Figure 5B–5E). To determine whether the higher subpopulation of cells expressing both P_{int} and P_{inR} -promoters was due to a generally higher level of RpoS in cells, we compared the RpoS-mCherry fluorescence levels in B13 with native *rpoS*_{B13} replaced by the *rpoS*_{B13-mcherry} allele (B13-3564) and in the same strain into which another single copy of *rpoS*_{B13-mcherry} was transposed (B13-3712). Indeed, the mean mCherry fluorescence in B13-3712 was almost twice as high as in B13-3564 (Figure 5F), suggesting that in double-copy *rpoS* strains on average more cells became permissive and could induce P_{inR} and P_{int} .

One extra copy of *rpoS* or *inrR* changes noise level in gene expression

In order to further examine how variability in RpoS levels would be linked to bistable expression of P_{inR} and P_{inb} , we measured the contribution of intrinsic and extrinsic noise on both promoters in individual cells. Noise was deduced from intra- and intercellular variations of reporter gene expression (eGFP and eCherry) from two individual single copy transcription fusions to P_{int} or P_{inR} , placed at different positions of the B13 chromosome as suggested in Elowitz *et al.* [39]. Fluorescence intensities from eGFP and eCherry were recorded in three independent clones with different insertion positions of the reporter fusion constructs to avoid positional effects as much as possible. Both markers essentially expressed in the same subpopulation of cells (Figure 6). Interestingly, the total noise was significantly higher on the P_{int} promoter than on P_{inR} (Table 4). Moreover, P_{int} expression was dominated by intrinsic rather than by extrinsic noise, which suggests that the variation in expression from P_{int} depends more strongly on variations in small numbers of regulatory molecules in individual cells, such as would be expected when P_{int} is at the end of a cascade involving InrR.

Adding an extra copy of *rpoS* or of *inrR* under control of their own promoters into the double- P_{int} reporter strain resulted in a significant decrease of intrinsic and total noise compared to wild-type (Table 4), which was insensitive to the size of the sampled

Table 3. Comparison of *rpoS* with double *inrR* deletion on eGFP expression from a single copy P_{int} -*egfp* fusion.

Time (h) ¹	A) <i>P. knackmussii</i> B13-1346 (wild-type)			B) B13-2976 (<i>rpoS</i>)			C) B13-2979 (<i>inrR</i> ^{-/-})	
	eGFP ²	% ³	signif ⁴	eGFP	%	signif	eGFP	%
24	68±7	1.1±0.1	AB, AC	<10	<0.1		<10	<0.1
48	96±1.4	2.2±0.1	AB, AC	47±3	0.4±0.1	BC	<10	<0.1
72	131±6	3.0±0.2	AB, AC	110±13	1.6±0.5	BC	94±7	0.4±1.2
96	143±6	3.4±0.1	AB, AC	140±16	2.1±0.4		63±7	1.2±0.8

¹Time after culture inoculation. Time 24 h is onset of stationary phase.

²Average eGFP fluorescence (relative units) within the subpopulation of ICE_{cl} active cells across biologically independent triplicates (for explanation, see Figure S7).

³Average subpopulation of cells (percent of total) expressing *egfp* from P_{int} , determined from cumulative distribution curves among biologically independent triplicates.

⁴Significance of difference (P<0.05) in a Tukey's post-hoc test on sample variances of subpopulation sizes per time group across all strains (one-way ANOVA).

doi:10.1371/journal.pgen.1002818.t003

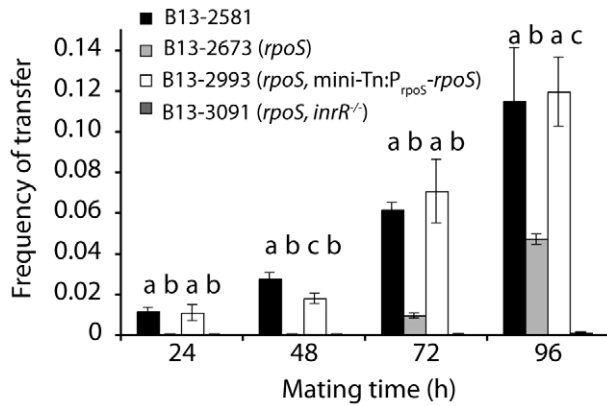


Figure 3. Effect of *rpoS* interruption on ICE clc transfer from *P. knackmussii* B13 to *P. putida* UWC1 as recipient as a function of mating time. Frequency of transfer expressed as number of transconjugant per number of donor colony forming units. Note that very low frequencies appearing on this scale as close to 'zero' are still detectable (exact values are given in Table S1). Letters above bar diagrams indicate significance of difference ($P < 0.05$) in a Tukey's post-hoc test on sample variances per mating time group (one-way ANOVA). doi:10.1371/journal.pgen.1002818.g003

subpopulation (Table S3). This indicates that the relative contribution of the extrinsic noise on P_{int} expression becomes more dominant, as would be expected from the increase in a global transcription factor (since RpoS is also directly acting on P_{int}). Also adding an additional copy of *inrR* resulted in a lowering of the total noise, although the proportion of cells expressing eGFP and eCherry in the *inrR*⁺ strain was not increased compared to wild-type (Figure 6, Table 4).

Discussion

One of the mysteries in ICE gene transfer among bacteria is the mechanism that controls the (typically low) frequency by which they become excised in clonally identical populations of donor cells. ICE conjugation must start with its excision and therefore the cellular decision that determines conjugation is binary: ICE excision or not. Low transfer frequencies (e.g., below 1% per donor cell in a population) suggest that the binary 'ON'-decision is only made in a very small proportion of donor cells. Indeed, our previous results on ICE clc in *P. knackmussii* B13 using stable fluorescent reporter gene fusions at single-cell level had indicated that 3% of cells in stationary phase after growth on 3-chlorobenzoate (3CBA) as sole carbon and energy source measurably express P_{inR} and P_{int} [8,33]. Moreover, single cell activation frequencies are in the same order as measured ICE clc excision and transfer at population level [33]. Our results presented here show for the first time how the expression level of the global transcription factor RpoS in individual cells across a population can modulate the frequency of cells activating excision of the ICE clc element.

By gene interruption and complementation we first establish that RpoS in *P. knackmussii* is a stationary phase sigma factor controlling transcription of the P_{inR} - and P_{int} -promoters and thus, indirectly, transfer of ICE clc to *P. putida*. Addition of an extra *rpoS*_{B13} gene copy led to an increased proportion of stationary phase cells in which the P_{inR} - and P_{int} -promoters are activated, which suggested that the expression level of RpoS is important for controlling the bistable switch leading to ICE clc activation. Indeed, by expressing an RpoS-mCherry fusion instead of RpoS wild-type protein in strain B13 we showed that P_{inR} - or P_{int} -*egfp* expression in

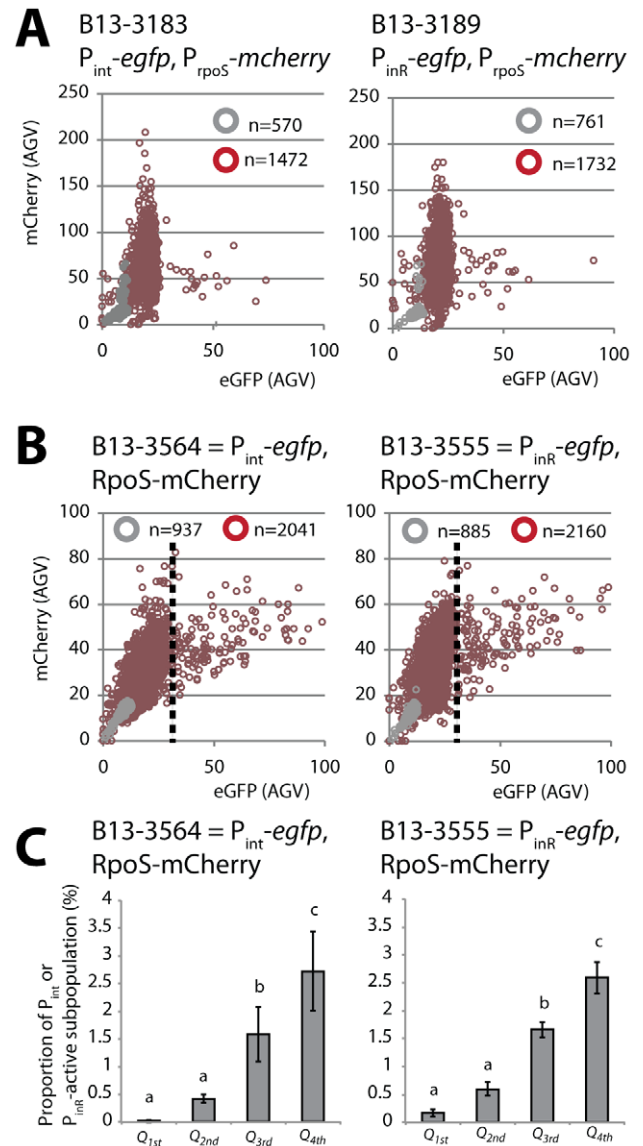


Figure 4. Correlation between *rpoS* and either P_{int} or P_{inR} expression in *P. knackmussii* B13. (A) Scatter plots of scaled single cell mCherry fluorescence expressed from P_{rpoS} and eGFP from P_{int} (left panel) or P_{inR} (right panel) in cultures on 3CBA in exponential phase (grey circles) or after 24 h in stationary phase (red-brown circles). (B) As A but showing single cell fluorescence of an RpoS-mCherry fusion protein (under transcriptional control from P_{rpoS}) versus eGFP fluorescence from P_{int} (left panel) or P_{inR} (right panel). Note that in strain B13-3564 and B13-3555 the native *rpoS* gene is replaced by *rpoS-mcherry*. Every circle represents measurements on a single cell. The total number of measured cells is displayed in every diagram. (C) Proportion of cells expressing eGFP above threshold (dotted lines in panel B) from P_{int} (left panel) or P_{inR} (right panel) in data sets of panel B per quadrant (Q) of normal distributed RpoS-mCherry intensity. Q_{1st} from minimum to Q_1 (mean-1 SD); Q_{2nd} from Q_1 to Q_2 (mean); Q_{3rd} from Q_2 to Q_3 (mean+1 SD); Q_{4th} from Q_3 to maximum. Letters above bar diagrams indicate significance of difference ($P < 0.05$) in a Tukey's post-hoc test on sample variances (one-way ANOVA). doi:10.1371/journal.pgen.1002818.g004

stationary phase preferably occurred in individual cells with the highest levels of RpoS-mCherry fluorescence (Figure 4C). Moreover, strains with two *rpoS-mCherry* gene copies produced on average twofold higher RpoS-mCherry protein fluorescence levels

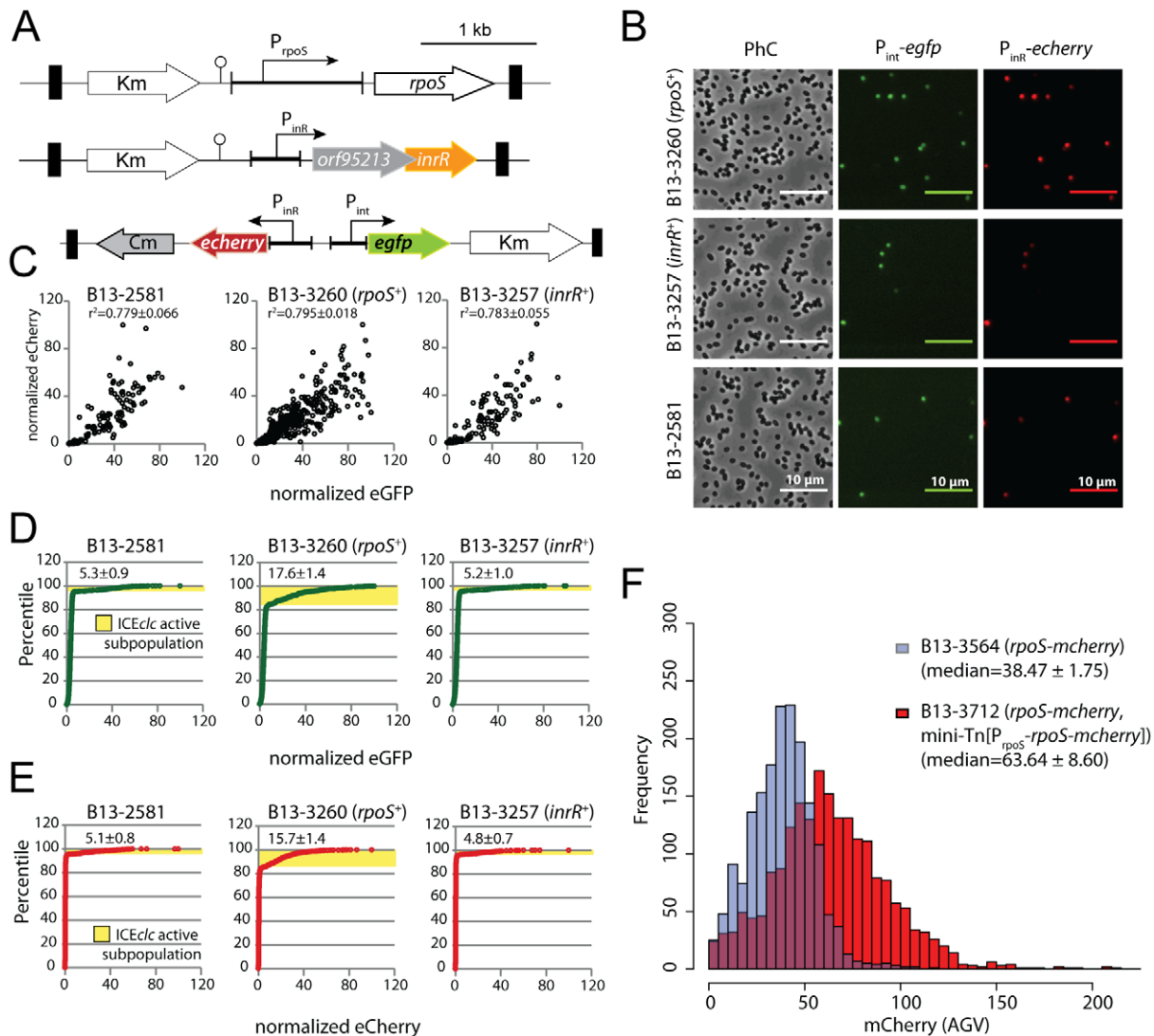


Figure 5. Effect of an additional copy of *rpoS* or *inrR* on the proportion of *P. knackmussii* B13 cells expressing P_{int} and P_{inR} in stationary phase. (A) Relevant construction details of the mini-transposon constructs used to deliver single copy *rpoS*, *inrR* or reporter genes. (B) Phase-contrast and corresponding epifluorescence micrographs (artificially colored green for eGFP and red for eCherry) of stationary phase cells grown on 3CBA at 1000 \times magnification. (C) Scatter plots showing correlation between normalized eGFP (from P_{inR}) and eCherry fluorescence (from P_{int}) in thousands of cells in B13-2581 (wild-type), B13-3260 (extra copy of *rpoS*) or B13-3257 (extra copy *inrR*). Correlation coefficients plus corresponding calculated standard deviations across biological triplicates are indicated. (D) Cumulative distributions of normalized eGFP fluorescence in strains of (C) and indication of the subpopulations of cells actively expressing P_{int} (average from triplicates \pm SD). (E) as (D), but for eCherry from P_{inR} . (F) Effect of an extra copy of *rpoS*-*mCherry* on the scaled RpoS-mCherry fluorescence levels in stationary phase cells. Shown are distributions of mCherry fluorescence in cultures of B13-3564 (*rpoS*-*mCherry* replaced *rpoS*, blue bars) and B13-3712 (*rpoS*-*mCherry* replaced *rpoS*, extra copy *rpoS*-*mCherry* on mini-Tn insertion, red bars). Median values plus corresponding calculated standard deviations across biological triplicates are indicated in parentheses.

doi:10.1371/journal.pgen.1002818.g005

in cells, leading to an increase of up to 20% of cells expressing eGFP from P_{inR} or P_{int} . This showed that an incidentally high RpoS level in an individual cell is a prerequisite for leading to P_{inR} - or P_{int} -expression. On the contrary, having a high RpoS-level is not sufficient and an as yet unknown other ICE clc -encoded factor(s) must be responsible for the activation or derepression of P_{inR} (Figure 7). We conclude that RpoS levels are a precondition for a cell or, in other words, a threshold, to activate the ICE clc bistable promoters during the first 2 days of stationary phase.

This conclusion is further supported by noise measurements on the P_{inR} or P_{int} -promoters (Figure 6). Intrinsic noise is dominant on the P_{int} promoter in wild-type B13, which would be in agreement

with the major role played by (a low abundant) InrR and the relatively minor role of (a widely abundant) RpoS directly on P_{int} -expression. This effect may actually have been overestimated by a bias introduced by the measurement technique (i.e., adding two extra P_{int} -copies with *egfp* or *mCherry* to two P_{int} from both ICE clc copies in the B13 chromosome, in the presence of two *inrR* copies). In contrast, and in the same 'biased' setting (two extra P_{inR} -copies on a total of four), the total noise is significantly lower on the P_{inR} -promoter and the relative contribution of the extrinsic noise is higher (Table 4), which is indicative for the more important contribution of RpoS on this promoter. Doubling the *rpoS* copy number resulted in a significant decrease of the total noise on P_{int}

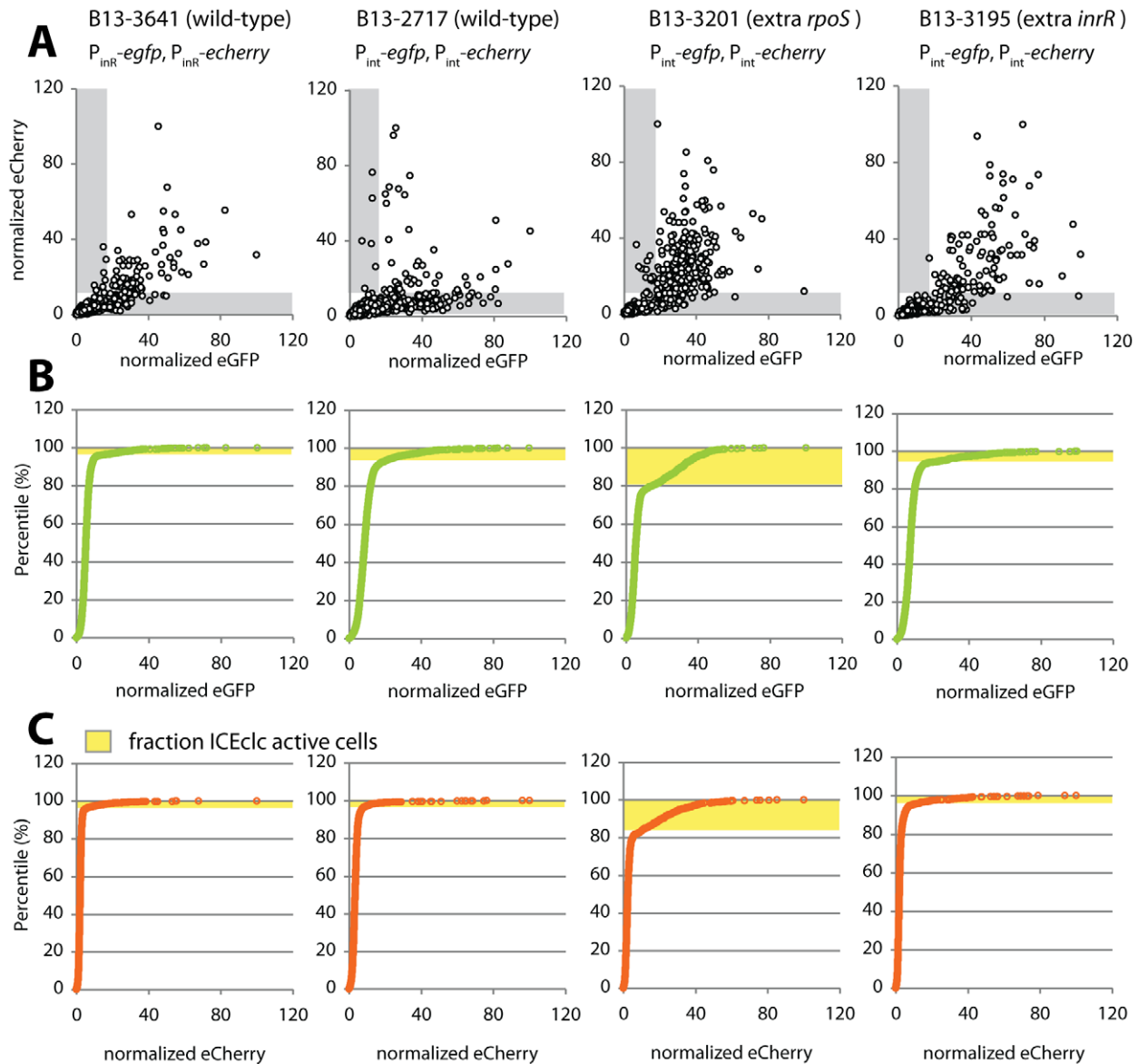


Figure 6. Noise in reporter gene expression from two separately placed single-copy identical promoters (P_{int} or P_{inR}) in *P. knackmussii* wild-type (strains 2717 and 3641) or with extra copies of *rpoS* (B13-3201) or *inrR* (B13-3195). (A) Scatter plots showing correlation between single cell scaled and normalized eCherry versus eGFP fluorescence values (circles) in stationary phase 3CBA-grown cultures. Grey zones indicate cells which express only one of both markers above threshold (for explanation, see Figure S8). (B) Cumulative distribution of single cell eGFP fluorescence values in the culture sample, used to define the subpopulation size of cells expressing eGFP from the P_{int} or P_{inR} promoters above threshold (in yellow). (C) as B, for the eCherry signals.
doi:10.1371/journal.pgen.1002818.g006

and a more important relative contribution of extrinsic noise (RpoS). This would make sense since individual cells would overall contain higher levels of RpoS permitting more direct interaction with P_{int} . Adding a third copy of *inrR* also reduced the level of intrinsic noise on P_{inR} , but in this case because such cells would produce more InrR, diminishing the noise effect by ‘small numbers’ of regulatory factors (i.e., InrR). Noise in individual cell RpoS levels is thus not propagated to noise in expression of downstream regulons, as was shown recently for global transcription factors in yeast [40], but rather is ‘captured’ in those cells having high RpoS levels and transduced by ICE clc factors to a precise activation cascade leading to ICE clc excision and transfer.

Intriguingly, doubling *rpoS* copy number strongly increased the proportion of cells in the population expressing P_{int} and P_{inR} from

3% to almost 20%, although the transfer frequency of ICE clc only doubled (Table S2). In contrast, adding a third copy of *inrR* to B13 did not statistically significantly increase the proportion of cells expressing P_{int} and P_{inR} . To explain this, we propose the following model for ICE clc bistability generation (Figure 7). In this model cells that by chance have the highest RpoS levels are pre-conditioned to activate ICE clc , although another factor is needed for the actual activation mechanism. Available data suggest that activation starts at P_{inR} , leading to synthesis of InrR, which, by an as yet unknown mechanism precisely relays activation (i.e., within the same individual cell) to P_{int} and other ICE clc core genes. Microarray analysis confirmed the important role of InrR for the overall activation of ICE clc core functions, and indicated a possible feedback loop on its own expression (Figure S6).

Table 4. Subpopulation proportions and noise in expression of eGFP and eCherry from dual P_{int} or P_{inR} fusions in cultures of *P. knackmussii* strain B13 or derivatives.

Strain	Marker	% fluorescent cells, eGFP ¹	% fluorescent cells, eCherry	Intrinsic noise	Extrinsic noise	Total noise
B13-2717	P_{int} - <i>egfp</i> , P_{int} - <i>echerry</i>	6.24 ± 0.87 (A) ²	4.24 ± 1.81 (A)	1.165 ± 0.128 (A)	0.304 ± 0.263	1.217 ± 0.174 (A)
B13-3641	P_{inR} - <i>egfp</i> , P_{inR} - <i>echerry</i>	4.01 ± 1.63 (A)	3.30 ± 0.71 (A)	0.547 ± 0.071 (B)	0.553 ± 0.091	0.779 ± 0.110 (B)
B13-3201 (extra <i>rpoS</i>)	P_{int} - <i>egfp</i> , P_{int} - <i>echerry</i>	19.85 ± 3.06 (B)	13.58 ± 5.86 (B)	0.572 ± 0.099 (B)	0.467 ± 0.029	0.739 ± 0.089 (B)
B13-3195 (extra <i>inrR</i>)	P_{int} - <i>egfp</i> , P_{int} - <i>echerry</i>	6.62 ± 0.4 (A)	5.53 ± 0.32 (A)	0.556 ± 0.034 (B)	0.488 ± 0.037	0.740 ± 0.050 (B)

¹Averages from three clones with different marker insertion positions ± calculated average deviation.

²Significantly different ($P < 0.05$) in a post-hoc Tukey's test calculated on sample variations in one-way ANOVA (per marker column across all strains).

doi:10.1371/journal.pgen.1002818.t004

Importantly, RpoS but not InrR levels determine the proportion of cells that may become ICE clc activated. The feedback loop of InrR on P_{inR} expression may be necessary to obtain sufficiently high InrR levels to act as co-regulator for the different ICE clc core gene operons [36]. Increasing *inrR* copy number, therefore, can decrease the noise in the expression of the ICE clc genes downstream of P_{inR} , but does not influence the proportion of cells in culture activating ICE clc . The fact that a double *rpoS* gene copy increases the number of cells expressing P_{int} and P_{inR} to 20% but only doubles transfer frequency suggests that there may be another component that is not under RpoS or InrR control that further limits conjugation rates. How may RpoS be accomplishing such a 'thresholding' control? One hypothesis is that RpoS has a relatively poor affinity for the P_{inR} -promoter and that, therefore, on average only cells with by chance high RpoS levels can activate P_{inR} . The *inrR* promoter bears a potential RpoS-motif in the -10 box (TGTCGATCCT), although it is not highly conserved [41].

As far as we are aware, this is the first time that RpoS has been implicated in controlling horizontal gene transfer of a conjugative element. RpoS homologs are part of a large protein cluster called the σ^{70} family, which is widely distributed among prokaryotes, although RpoS regulons can be quite different in individual species [42]. The only other report detailing a role for RpoS dealt with stationary phase regulation of Tn4652 activity in *P. putida* [43]. Interestingly, in that case RpoS downregulates *tnpA* transposition

frequency since Tn4652 becomes at least 10 times more activated in an *rpoS*-defective strain [43]. Study on effects of stochastic fluctuations in sigma factors at the single cell level are extremely limited. Perez-Osorio documented highly heterogeneous *rpoS* mRNA levels in *P. aeruginosa* biofilms, but this occurred rather as a consequence of physico-chemical gradients within the biofilm [44]. Stochastic stress-induced fluctuations control the *rbsV-rbsW-sigB* operon for the stress response sigma factor SigB in *Bacillus subtilis*. Interestingly, *sigBp* expression proceeds in a 'burst-like' fashion with a higher pulse frequency under stress than under normal growth condition [45]. Bursts are initiated by stress-dependent fluctuations in phosphatase levels, then first amplified and subsequently terminated by *sigB* operon feedback on itself and on its anti- and anti-anti-sigma factors RbsW and RbsV, respectively.

Gene expression noise is ubiquitous and plays an essential role in a variety of biological processes, triggering stochastic differentiation in clonal populations of cells [46]. Noise can provide a selective advantage by increasing phenotypic heterogeneity and increasing the chance of individuals to survive [46]. Evidence exists that more noisy systems can become selected under specific conditions [47]. In that sense, our data implicate that specific evolutionary elements such as ICE clc are wired within noise in a global transcription factor but can transduce this noise to a precise activation cascade, and thus may have been selected for their capacity to successfully exploit the noise.

Materials and Methods

Bacterial strains and plasmids

Escherichia coli DH5 α (Gibco Life Technologies, Gaithersburg, Md.) was routinely used for plasmid propagation and cloning experiments. *E. coli* HB101 (pRK2013) was used as helper strain for conjugative delivery of mini-transposon constructs [48]. *P. knackmussii* strain B13 [49] is the original host of the *clc* element (ICE clc), of which it carries two copies [50]. All further B13 derivatives are listed in Table 1.

Media and growth conditions

Luria-Bertani (LB) medium [51] was used for cultivation of *E. coli*, whereas LB and type 21C mineral medium (MM) [52] were used for cultivation of *P. knackmussii*. 3-Chlorobenzoate (3CBA) was added to MM to a final concentration of 5 or 10 mM. When necessary, the following antibiotics were used at the indicated concentrations ($\mu\text{g per ml}$): ampicillin, 500 (for *P. knackmussii*) or 100 (for *E. coli*); kanamycin, 50 and tetracycline, 100 (for *P. knackmussii* strain B13 derivatives) or 12.5 (for *E. coli*). *P. knackmussii* strain B13 was grown at 30°C; *E. coli* was grown at 37°C.

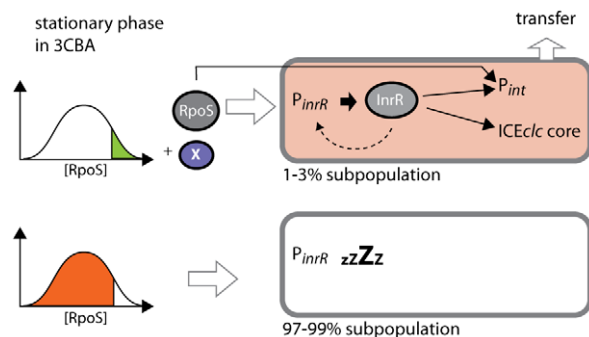


Figure 7. Stochastic fluctuations of RpoS control permissiveness for bistable ICE clc activation and transfer. Stationary phase cells grown on 3CBA with the highest cellular RpoS levels and in the presence of the regulator(s) factor X can activate P_{inR} . InrR positively controls the expression of P_{int} and other ICE clc core genes, finally leading to ICE clc transfer. A positive feedback loop by InrR may lead to higher InrR expression, but only in ICE clc active cells. RpoS is also a direct sigma factor for P_{int} -expression. Cells with lower RpoS levels do not express P_{inR} and ICE clc remains non-active.
doi:10.1371/journal.pgen.1002818.g007

ICE clc self-transfer

Self-transfer was tested by mixing 500 μ l suspension of around 10^9 donor cells (*P. knackmussii* B13 or one of its derivatives) and 500 μ l suspension of around 10^9 recipient cells (*P. putida* UWC1) on membrane filters for 24, 48, 72 or 96 h, as described earlier [53]. Transconjugants (*P. putida* UWC1 with ICE clc) were selected on MM plates with 5 mM 3CBA as sole carbon and energy source (to select for ICE clc) and 50 μ g per ml rifampicin (resistance marker of the recipient). Transfer frequencies were expressed as number of transconjugant colony forming units (CFU) per number of donor CFU.

DNA and RNA techniques

Polymerase chain reaction (PCR), reverse transcription RT-PCR, plasmid and chromosomal DNA isolations, RNA isolation, DNA fragment recovery, DNA ligations, transformations into *E. coli* and restriction enzyme digestions were all carried out according to standard procedures [51] or to specific recommendations by the suppliers of the molecular biology reagents (Qiagen GmbH; Promega; Stratagene). Sanger-type DNA sequencing was performed on an automated DNA sequencer using a 3.1 Big-Dye kit (Applied Biosystems, ABI PRISM, 3100 DNA sequencer). Sequences were aligned and verified with the help of the Lasergene software package (Version 7, DNASTAR Inc., Madison, Wisc.). Sequence databases were interrogated by using the BLAST program [54].

Cloning of *rpoS* from *P. knackmussii* B13

Primers were designed for conserved regions obtained in a nucleotide sequence alignment among *rpoS* genes of *P. aeruginosa*, *P. putida* and *P. fluorescens* (Table S4, Figure S1). A single 1-kb PCR product was obtained using these primers and B13 genomic DNA as template. This fragment was cloned and sequenced on both strands by primer walking. Surrounding regions of the *rpoS* gene of *P. knackmussii* were retrieved from draft genome sequence of *P. knackmussii* B13 (R. Miyazaki and J. R. van der Meer, unpublished). The B13 *rpoS* gene region was submitted to GenBank under accession number AB696604.

RpoS disruption

An internal fragment of the *rpoS*_{B13} gene was amplified with a forward primer (080304) carrying a *Bam*HI, and reverse primer (080303) carrying an *Eco*RI restriction site (Table S4). The amplified fragment was digested and cloned into the suicide plasmid vector pME3087, which carries a tetracycline resistance [55]. The plasmid was then mobilized from *E. coli* into *P. knackmussii* strain B13 via conjugation. Potential B13 transconjugants with a single recombination into *rpoS* were selected on MM with 5 mM 3CBA as carbon source plus 100 μ g per ml tetracycline, further purified by replating and verified by PCR for accuracy of homologous recombination. In this manner a mutant of strain B13 was obtained in which *rpoS* was replaced by two incomplete and separated *rpoS* fragments (Figure S3). This mutant was named B13 *rpoS* (strain 2671). Separate experiments to delete *rpoS* by using recombination with a DNA fragment in which *rpoS* was fully deleted were not successful either (not shown). The same strategy was then used to produce a single recombinant disruption of *rpoS* in *P. knackmussii* strain B13 that lacked both *inrR* copies [33]. Reversion of the *rpoS*-pME3087 allele to wild-type *rpoS* in stationary phase cultures was tested by specific PCR (Table S4, Figure S4B).

rpoS complementation

A 2.2-kbp fragment containing the *rpoS* gene and its presumed promoter (P_{rpoS}) was amplified from strain B13 purified genomic DNA using primers 091206 and 090902 (Table S4). The amplified material was first cloned into the vector pGEM-T-Easy (Promega). From here, the P_{rpoS} -*rpoS* fragment was recovered by *Not*I digestion and inserted into the mini-Tn5 delivery plasmid pCK218, which was used to place the construction in single copy on the chromosome of strain B13-2673 (*rpoS*, mini-Tn[P_{inrR} -*echerry-cat*, P_{int} -*egfp*, Km], see below). As this strain carried a mini-Tn5 insertion already it was necessary to remove the Km gene cassette associated with it. Hereto the strain was transformed with plasmid pTS-parA [56], a temperature-sensitive replicon transiently expressing the ParA resolvase. B13 transformants were selected on LB plus ampicillin and subsequently grown in the absence of kanamycin for twelve generations. Clones that had lost the Km cassette were screened by replica plating and the absence of the gene was verified by PCR. Finally, the temperature sensitive replicon was cured by growing the strain in LB at 37°C for 16 h and ensuring ampicillin sensitivity. The resulting strain was then used to introduce the mini-Tn5 containing the P_{rpoS} -*rpoS* fragment, which was designated B13-2993 (*rpoS*, mini-Tn[P_{rpoS} -*rpoS*, Km], mini-Tn[P_{inrR} -*echerry-cat*, P_{int} -*egfp*]). Three independent clones with possible different mini-transposon insertion sites were examined for ICE clc transfer and reporter gene expression.

Extra-copy of *inrR* and *rpoS*

A 1700-bp fragment containing *orf95213* and *inrR* genes plus P_{inrR} was amplified by PCR using primers (060605+080502, Table S4) carrying *Eco*RI and *Spe*I restriction sites, respectively. The P_{inrR} -*orf95213*-*inrR* fragment was digested with *Eco*RI and *Spe*I and cloned into the mini-Tn5 delivery plasmid pBAM1 [57]. In the same way, a 2.2-kb fragment containing P_{rpoS} -*rpoS* was amplified with primers (091206+090902) and cloned in pBAM1 using *Sph*I and *Eco*RI. The resultant suicide plasmids were introduced into B13 or its derivatives by electroporation, from where the transposition was selected by plating on MM plus 3CBA and kanamycin. *Bona fide* single copy transposition was verified by PCR. At least three independent clones with possibly different insertion positions were used for further experiments.

Promoter-reporter gene fusions

Transcriptional fusions between the P_{int} promoter in front of *intB13* and the *egfp* gene, or P_{int} and a promoterless *echerry* gene have been described previously [33,58]. Transcriptional fusion between the promoter of the *orf95213*, *inrR*, *ssb* gene cluster (P_{inrR}) and either *egfp* or *echerry* have been detailed elsewhere [33]. To examine expression of both P_{inrR} and P_{int} promoters simultaneously, we used a previous construct with P_{inrR} -*echerry* in one and P_{int} -*egfp* in the opposite direction [33]. Fusions were inserted in single copy into the chromosome of strain B13 or its mutant derivatives via mini-Tn5 delivery using pCK218 [59]. To measure activity of the *rpoS* promoter (P_{rpoS}), a 1200-bp fragment upstream of *rpoS* including the *nlpD* gene was amplified from strain B13 by PCR (Figure 1). This fragment was purified and digested with *Not*I and *Eco*RI, and unidirectionally fused to a promoterless *mcherry* gene in the mini-Tn5 vector pBAM1 [57]. Transposon insertion mutants were selected on MM with 3CBA plus kanamycin or tetracycline and purified, upon which the correctness of the mini-Tn5 insertion was verified by PCR. For all mini-transposon insertions at least three independent clones were purified and examined for induction.

Translational fusions of RpoS with mCherry

To produce a C-terminal fusion of RpoS to mCherry, a ~750 bp fragment containing the *mcherry* open reading frame was amplified using pMQ64-mcherry (kindly obtained from Dianne Newman, CalTech) as a template and primers (101003 and 101004), in which the start codon of *mcherry* was replaced by a short nucleotide sequence encoding 15 amino acids (KLPENSNVTRHRSAT) as a linker peptide. The fragment was then cloned in *Hind*III and *Spe*I sites on the mini-Tn5 delivery plasmid pBAM1, resulting in pBAM-link-mCherry. A 2.1 kb region containing P_{rpoS} and *rpoS* lacking its stop codon was amplified using B13 genomic DNA and primers 101001 plus 010102. This fragment was digested with *Eco*RI and *Hind*III, and cloned into the same sites on pBAM-link-mCherry (designated pBAM-rpoS-mcherry). After transformation in *E. coli* and purification, this plasmid was introduced into strain B13 or its derivatives by electroporation. Single copy transposon insertions of the *rpoS-mcherry* fusion construct were selected by plating cells on MM plus 3CBA and kanamycin. If required for introduction of subsequent mini-transpositions the kanamycin gene cassette was removed by ParA resolvase action (see above). At least three independent clones with possibly different insertion positions were used for further experiments.

To replace *rpoS* of B13 by the gene for the RpoS-mCherry fusion protein we used double recombination by crossing-over. Hereto, a ~1 kb downstream region of *rpoS* was first amplified using B13 genomic DNA and primers 110524 plus 110525, which was digested using *Xba*I and *Sal*I and ligated with pJP5603-ISceIv2 [60]. Next, the gene for the RpoS-mCherry translational fusion protein on pBAM-rpoS-mcherry was recovered by digestion with *Eco*RI and *Spe*I, an inserted upstream of the amplified fragment in pJP5603-ISceIv2 which was hereto digested with *Eco*RI and *Xba*I. After transformation in *E. coli* and purification, the resulting plasmid was electroporated into strain B13-78 (Table 1). Single and double recombinants were selected according to a previously described strategy [9], obtaining an allelic exchange mutant that has the gene for RpoS-mCherry instead of the original *rpoS*.

Fluorimeter measurements

P. knackmussii strain B13 or B13 *rpoS* carrying the P_{rpoS-mcherry} fusion were grown in 96-well black microtiter plates (Greiner Bio-one) with a flat transparent bottom. Each well contained 200 µl of MM medium with 5 mM 3CBA and was inoculated with 2 µl of a bacterial preculture grown overnight in LB medium. Microtiter plates were incubated at 30°C with orbital shaking at 500 rpm. At each given time point both culture turbidity (A₆₀₀) and fluorescence emission (excitation at 590 nm and emission at 620 nm) were measured from triplicate cultures using a Fluostar fluorescence microplate reader (BMG Lab Technologies). Cultures of *P. knackmussii* strain B13-78 wild-type served for background fluorescence correction.

Epifluorescence microscopy

To image eGFP, eCherry or mCherry expression in single cells, culture samples of 4 µl were placed on regular microscope slides, closed with a 50 mm long and 0.15 mm thick cover slip, and imaged within 1–2 minutes. Fluorescence intensities of individual cells were recorded on image fields not previously exposed to UV-light to avoid bleaching. For most imaging series, except data shown in Figure 2, a Zeiss Axioskop2 upright epifluorescence microscope was used, equipped with Spot Xplorer 1.4MPixel cooled CCD camera (Visitron Systems GmbH, Puchheim,

Germany), and 100×/1.30 oil immersion Plan-Neofluar lens at an exposure time of 500 ms. Filters used for eGFP and for eCherry/mCherry were eGFP HQ470/40 and Cy3 HQ545/30, respectively (Chroma Technology Corp, VT, USA). Images were digitally recorded using VisiView software (version 2.0.4, Visitron Systems GmbH). For data shown in Figure 2 and Figure S3 a Leica DMI6000B inverted epifluorescence microscope was used, equipped with a cooled black-and-white charge-coupled device camera (DFC320, Leica Microsystems CMS GmbH, Wetzlar, Germany), a 100/1.30 oil immersion lens (HCX PL FLUOTAR; Leica), at an exposure time of 800 ms. Filters used for eGFP, and for eCherry or mCherry were GFP BP470/40 and Y3 BP535/50, respectively (Leica). Images were digitally recorded as 8-bit TIFF-files using the Leica AF6000 software. The mean pixel intensity for every individual object in an image was quantified by an automatic subroutine in the program MetaMorph (version 7.7.5; Visitron Systems GmbH) as described previously [33]. Fluorescence intensities per cell were expressed as cellular average gray values (AGVs) in which background intensities of each image were subtracted.

Subpopulation expression was determined from cumulative ranking of all objects according to their AGV. The ‘breakpoint’ between subpopulations on cumulative distribution curves (Figure S8) was determined by manually placing slope lines to the linear parts of the curve. The point where both slope lines crossed was used to determine the corresponding percentile for the largest subpopulation with lowest AGVs. The relative size of the subpopulation with highest AGVs (indicative for bistable promoter expression of P_{int} and P_{inR}) was then calculated as 100% - the percentile of the breakpoint. The average expression intensity over the highest expressing subpopulation was calculated as the mean AGV over the percentile range between that of the breakpoint and 100%. Fluorescence images for display were adjusted for brightness to a level +143, cropped to their final size and saved at 300 dpi with Adobe Photoshop (Version CS4). Corresponding phase-contrast images were ‘auto contrasted’ using Photoshop.

Noise calculation

To identify and quantify noise in expression of the P_{int} and P_{inR} promoters, two identical copies were fused to distinguishable reporter genes (i.e. *egfp* and *echerry*) and integrated into separate locations on the chromosome of B13 or its derivatives using mini-Tn5 delivery. Three independent clones with different insertional positions were maintained. Stationary phase cells of such double-reporter strains grown in MM with 3CBA were examined in epifluorescence microscopy, and their eGFP and eCherry fluorescence intensities were measured as outlined above (AGVs). AGVs of both markers in each cell were scaled to subtract background AGV of digital EFM images and normalized to the highest AGV in a population (100%). Only cells belonging to the subpopulations of having higher eGFP or eCherry fluorescence than the breakpoint in the respective cumulative curves (e.g., Figure 6) were used for noise calculation. Intrinsic noise (η_{int}), extrinsic noise (η_{ext}), and total noise (η_{tot}) were then calculated according to previous definitions given in Elowitz *et al.* [40] as follows:

$$\eta_{int}^2 \equiv \frac{\langle (g-c)^2 \rangle}{2\langle g \rangle \langle c \rangle}; \quad \eta_{ext}^2 \equiv \frac{\langle gc \rangle - \langle g \rangle \langle c \rangle}{\langle g \rangle \langle c \rangle}; \quad \eta_{tot}^2 \equiv \frac{\langle g^2 + c^2 \rangle - 2\langle g \rangle \langle c \rangle}{2\langle g \rangle \langle c \rangle}$$

where *g* and *c* denote the normalized eGFP and eCherry AGV, respectively, observed in the *n*th single cell. Angled brackets denote a mean over the sample population.

Statistics

Significance of different treatments was examined by pair-wise t-test or ANOVA followed by a Tukey post hoc test. To test the effect of subpopulation size on noise calculations, data sets were randomly resampled using bootstrap procedures (1000 times), upon which the intrinsic, extrinsic and total noise were calculated and finally, averaged over all resampled populations of the same data set.

Microarray analysis

Total RNA was isolated from *P. knackmussii* B13-78 (wild type), B13-2671 (*rpoS*) and B13-2201 (*inrR*^{-/-}) cultures after 48 h in stationary phase after growth on 3CBA as sole carbon and energy source, by using the procedure described previously [37]. Briefly, cDNA was synthesized from total RNA, labeled with cyanine-3, purified and hybridized to a 8×15K custom-made Agilent microarray chip (Agilent Technologies, Santa Clara, CA). Data analysis was performed as described previously [37]. Microarray data and design have been deposited in the NCBI Gene Expression Omnibus (GEO) under accession number GPL10091.

Supporting Information

Figure S1 Alignment of *rpoS* genes from *Pseudomonas putida* (*P. p.*), *P. fluorescens* (*P. f.*) and *P. aeruginosa* (*P. a.*). Rectangular boxes represent the region chosen to design primers for the amplification of *rpoS* from strain B13. Inosine was used in the oligonucleotides at non-conserved positions. Genbank numbers: *P. putida* KT2440, NC_002947.3; *P. fluorescens* PF-5, NC_004129.6; *P. aeruginosa* PAO1, NC_002516.2. (TIF)

Figure S2 Comparison of the predicted RpoS amino acid sequence from strain B13 and orthologues from four other *Pseudomonas* strains. (A) MegAlign alignment (DNASar LaserGene package v.8) and indication of consensus per position. (B) Dendrogram (Clustal 2.0.12, <http://www.ebi.ac.uk>) showing the closest neighbourhood clustering of the strain B13 *rpoS* gene. (TIF)

Figure S3 Strategy for inactivating *rpoS* in strain B13 by a single recombination event. (A) *rpoS* gene region. (B) Amplification of a 600-bp internal *rpoS*_{B13} fragment by PCR whilst creating *Bam*HI and *Eco*RI restriction sites. Insertion of the *rpoS*_{B13} fragment into the suicide vector pME3087. (C) Genetic structure produced by single homologous recombination and inactivation of *rpoS* on the B13 chromosome. (TIF)

Figure S4 Growth of *P. knackmussii* B13-78 wild-type and B13-2671 (*rpoS*) in MM with 5 mM 3CBA. Data points are the average from three independent biological replicates ± one calculated standard deviation. Maximal specific growth rates in exponential phase for B13-78 were 0.22±0.01 versus 0.26±0.01 h⁻¹ for B13-2671 (*rpoS*). Note that growth medium for B13-2671 included Tc to select for the *rpoS*-pME3087 allele. (B) Semi-quantification of the presence of *rpoS* revertants in B13-2671 (*rpoS*) cultures by PCR. 25 ng of genomic DNAs isolated from B13-2671 culture with Tc at 24 h (lane 5), 48 h (lane 6), 72 h (lane 7), or 96 h (lane 8) were used as templates. A serially diluted B13-78 (wild-type) DNA was used as control: lane 1, 0.25 ng; lane 2, 0.5 ng; lane 3, 2.5 ng; lane 4, 25 ng. Intact *rpoS* (upper panel) and *fdxA* (lower panel, as an internal control) alleles were amplified using primer pairs 090206+090902 and 110524+110525, respectively. Lane M,

molecular mass marker (MassRuler DNA Ladder, Fermentas). The positions and sizes of the expected PCR fragments are indicated. Note that some reversion of *rpoS*-pME3087 to wild-type *rpoS* must occur (lane 7–9) but at less than 1% in the population (lane 1). (TIF)

Figure S5 Comparison of effects caused by *rpoS* or double *inrR* disruption on expression of a P_{inr-egfp} fusion in *P. knackmussii*. (A) Relevant construction details of the mini-Tn construct delivering the single copy P_{inr-egfp} fusion. (B) Micrographs showing the subpopulation of cells expressing eGFP from P_{inr} amidst a large number of silent cells for B13-1346 (wild-type), B13-2976 (*rpoS*) or B13-2979 (*inrR*^{-/-}) cultured on 3CBA after 24 h into stationary phase. (C) As B, but after 72 h in stationary phase. Shown are phase-contrast micrographs at 1,000× magnification and corresponding epifluorescence images. For quantification, see Table 3. (TIF)

Figure S6 ICE clc gene expression compared among *P. knackmussii* B13-78 (wild-type), B13-2201 (*inrR*^{-/-}) and B13-2671 (*rpoS*). (A) Log₂ fold-change in negative-strand probe signals on an ICE clc micro-array. Inset shows detail around *inrR*-operon. (B) Positive-strand probe signals. Open reading frames of ICE clc plotted along its length; white boxes: genes oriented on the positive strand, grey boxes: negative strand. Known ICE clc functional genes or regions indicated by name for reference. (TIF)

Figure S7 Growth phase dependent expression from the *rpoS* promoter in *P. knackmussii*. (A) Relevant construction details of the mini-Tn construct used to place a single copy P_{rpoS-mCherry} transcriptional fusion in the B13 genome. (B) Culture-density normalized mCherry fluorescence as a function of culture density (open circles) and incubation time in B13-3165 (wild-type) B13-3228 (*rpoS*), or B13-3654 (*rpoS*-mCherry). (C) Corresponding phase contrast (PhC) and epifluorescence micrographs of B13-3165 cells 24 h into stationary phase. Note how expression from P_{rpoS} is RpoS independent and how expression of RpoS-mCherry from P_{rpoS} is detectable slightly later than that of mCherry alone, suggesting post-transcriptional effects. (TIF)

Figure S8 Calculation of the subpopulation (size and mean reporter fluorescence expression) of B13-cells expressing P_{inr} or P_{inr} above threshold and representative for activating the ICE clc element. (A) Finding the breakpoint between the larger non-active subpopulation of cells and the smaller ICE clc -active subpopulation of cells on a cumulative distribution curve of reporter fluorescence values from P_{inr} or P_{inr}. (B) Scaling and normalizing of eCherry and eGFP expression for noise calculations. Only cells falling in the grey zones (i.e., those with reporter expression values above the threshold defined in [A]) are considered for noise calculation. (TIF)

Table S1 Transfer frequencies of ICE clc from *P. knackmussii* strain B13, the *inrR* deletion and the *rpoS* deletion mutants to *P. putida* UWC1 as recipient. (DOC)

Table S2 Transfer frequencies of ICE clc from *P. knackmussii* strain B13 and the *rpoS*⁺ strain to *P. putida* UWC1 as recipient. (DOC)

Table S3 Effect of subpopulation size on noise calculation from two identical P_{int} -copies in different places on the chromosome of *P. knackmussii* derivatives. (DOC)

Table S4 Primers used in this study. (DOC)

References

- Juhas M, van der Meer JR, Gaillard M, Harding RM, Hood DW, et al. (2009) Genomic islands: tools of bacterial horizontal gene transfer and evolution. *FEMS Microbiol Rev* 33: 376–393.
- Wozniak RA, Waldor MK (2010) Integrative and conjugative elements: mosaic mobile genetic elements enabling dynamic lateral gene flow. *Nat Rev Microbiol* 8: 552–563.
- Burrus V, Waldor MK (2004) Shaping bacterial genomes with integrative and conjugative elements. *Res Microbiol* 155: 376–386.
- Dobrindt U, Hochhut B, Hentschel U, Hacker J (2004) Genomic islands in pathogenic and environmental microorganisms. *Nat Rev Microbiol* 2: 414–424.
- Sentchilo V, Czechowska K, Pradervand N, Minoia M, Miyazaki R, et al. (2009) Intracellular excision and reintegration dynamics of the ICE c genomic island of *Pseudomonas knackmussii* sp. strain B13. *Mol Microbiol* 72: 1293–1306.
- Beaber JW, Hochhut B, Waldor MK (2004) SOS response promotes horizontal dissemination of antibiotic resistance genes. *Nature* 427: 72–74.
- Auchtung JM, Lee CA, Monson RE, Lehman AP, Grossman AD (2005) Regulation of a *Bacillus subtilis* mobile genetic element by intercellular signaling and the global DNA damage response. *Proc Natl Acad Sci U S A* 102: 12554–12559.
- Sentchilo VS, Ravatn R, Werlen C, Zehnder AJB, van der Meer JR (2003) Unusual integrase gene expression on the *clc* genomic island of *Pseudomonas* sp. strain B13. *J Bacteriol* 185: 4530–4538.
- Miyazaki R, van der Meer JR (2011) A dual functional origin of transfer in the ICE c genomic island of *Pseudomonas knackmussii* B13. *Mol Microbiol* 79: 743–758.
- Williams KP (2002) Integration sites for genetic elements in prokaryotic tRNA and tmRNA genes: sublocation preference of integrase subfamilies. *Nucleic Acids Res* 30: 866–875.
- Nunes-Duby SE, Kwon HJ, Tirumalai RS, Ellenberger T, Landy A (1998) Similarities and differences among 105 members of the Int family of site-specific recombinases. *Nucleic Acids Res* 26: 391–406.
- Beaber JW, Hochhut B, Waldor MK (2002) Genomic and functional analyses of SXT, an integrating antibiotic resistance gene transfer element derived from *Vibrio cholerae*. *J Bacteriol* 184: 4259–4269.
- Mohd-Zain Z, Turner SL, Cerdeño-Tarraga AM, Lilley AK, Inzana TJ, et al. (2004) Transferable antibiotic resistance elements in *Haemophilus influenzae* share a common evolutionary origin with a diverse family of syntenic genomic islands. *J Bacteriol* 186: 8114–8122.
- Shoemaker NB, Vlamakis H, Hayes K, Salyers AA (2001) Evidence for extensive resistance gene transfer among *Bacteroides* spp. and among *Bacteroides* and other genera in the human colon. *Appl Environ Microbiol* 67: 561–568.
- Schubert S, Dufke S, Sorsa J, Heesemann J (2004) A novel integrative and conjugative element (ICE) of *Escherichia coli*: the putative progenitor of the *Yersinia* high-pathogenicity island. *Mol Microbiol* 51: 837–848.
- He JX, Baldini RL, Deziel E, Saucier M, Zhang QH, et al. (2004) The broad host range pathogen *Pseudomonas aeruginosa* strain PA14 carries two pathogenicity islands harboring plant and animal virulence genes. *Proc Natl Acad Sci U S A* 101: 2530–2535.
- Bordeleau E, Brouillette E, Robichaud N, Burrus V (2010) Beyond antibiotic resistance: integrating conjugative elements of the SXT/R391 family that encode novel diguanylate cyclases participate to c-di-GMP signalling in *Vibrio cholerae*. *Environ Microbiol* 12: 510–523.
- Sullivan JT, Ronson CW (1998) Evolution of rhizobia by acquisition of a 500-kb symbiosis island that integrates into a phe-tRNA gene. *Proc Natl Acad Sci U S A* 95: 5145–5149.
- Gross R, Guzman CA, Sebahia M, dos Santos VA, Pieper DH, et al. (2008) The missing link: *Bordetella petrii* is endowed with both the metabolic versatility of environmental bacteria and virulence traits of pathogenic *Bordetellae*. *BMC Genomics* 9: 449.
- Chain PS, Denef VJ, Konstantinidis KT, Vergez LM, Agullo L, et al. (2006) *Burkholderia xenovorans* LB400 harbors a multi-replicon, 9.73-Mbp genome shaped for versatility. *Proc Natl Acad Sci U S A* 103: 15280–15287.
- Gaillard M, Vallaeyts T, Vorholter FJ, Minoia M, Werlen C, et al. (2006) The *clc* element of *Pseudomonas* sp. strain B13, a genomic island with various catabolic properties. *J Bacteriol* 188: 1999–2013.
- Miyazaki R, Minoia M, Pradervand N, Sentchilo V, Sulser S, et al. (2011) The *clc* element and related genomic islands in *Proteobacteria*. In: Roberts AP, Mullany P, editors. *Bacterial integrative mobile genetic elements*: Landes Bioscience.
- Klockgether J, Würdemann D, Reva O, Wiehmann L, Tümmler B (2007) Diversity of the abundant pKLC102/PAGI-2 family of genomic islands in *Pseudomonas aeruginosa*. *J Bacteriol* 189: 2443–2459.
- Mathee K, Narasimhan G, Valdes C, Qiu X, Mawehish JM, et al. (2008) Dynamics of *Pseudomonas aeruginosa* genome evolution. *Proc Natl Acad Sci U S A* 105: 3100–3105.
- Daccard A, Ceccarelli D, Burrus V (2010) Integrating conjugative elements of the SXT/R391 family trigger the excision and drive the mobilization of a new class of *Vibrio* genomic islands. *Mol Microbiol* 78: 576–588.
- Boyd EF, Cohen AL, Naughton LM, Ussery DW, Binnewies TT, et al. (2008) Molecular analysis of the emergence of pandemic *Vibrio parahaemolyticus*. *BMC Microbiol* 8: 110.
- Kettler GC, Martiny AC, Huang K, Zucker J, Coleman ML, et al. (2007) Patterns and implications of gene gain and loss in the evolution of *Prochlorococcus*. *PLoS Genet* 3: e231. doi:10.1371/journal.pgen.0030231
- Kung VL, Ozer EA, Hauser AR (2010) The accessory genome of *Pseudomonas aeruginosa*. *Microbiol Mol Biol Rev* 74: 621–641.
- Beaber JW, Waldor MK (2004) Identification of operators and promoters that control SXT conjugative transfer. *J Bacteriol* 186: 5945–5949.
- Bose B, Auchtung JM, Lee CA, Grossman AD (2008) A conserved anti-repressor controls horizontal gene transfer by proteolysis. *Mol Microbiol* 70: 570–582.
- Bellanger X, Roberts AP, Morel C, Choulet F, Pavlovic G, et al. (2009) Conjugative transfer of the integrative conjugative elements ICES $t1$ and ICES $t3$ from *Streptococcus thermophilus*. *J Bacteriol*.
- Losick R, Desplan C (2008) Stochasticity and cell fate. *Science* 320: 65–68.
- Minoia M, Gaillard M, Reinhard F, Stojanov M, Sentchilo V, et al. (2008) Stochasticity and bistability in horizontal transfer control of a genomic island in *Pseudomonas*. *Proc Natl Acad Sci U S A* 105: 20792–20797.
- Dubnau D, Losick R (2006) Bistability in bacteria. *Mol Microbiol* 61: 564–572.
- Veening JW, Stewart EJ, Berngruber TW, Taddei F, Kuipers OP, et al. (2008) Bet-hedging and epigenetic inheritance in bacterial cell development. *Proc Natl Acad Sci U S A* 105: 4393–4398.
- Gaillard M, Pradervand N, Minoia M, Sentchilo V, Johnson DR, et al. (2010) Transcriptome analysis of the mobile genome ICE c in *Pseudomonas knackmussii* B13. *BMC Microbiol* 10: 153.
- Schuster M, Hawkins AC, Harwood CS, Greenberg EP (2004) The *Pseudomonas aeruginosa* RpoS regulon and its relationship to quorum sensing. *Mol Microbiol* 51: 973–985.
- Suh SJ, Silo-Suh L, Woods DE, Hassett DJ, West SE, et al. (1999) Effect of *rpoS* mutation on the stress response and expression of virulence factors in *Pseudomonas aeruginosa*. *J Bacteriol* 181: 3890–3897.
- Elowitz MB, Levine AJ, Siggia ED, Swain PS (2002) Stochastic gene expression in a single cell. *Science* 297: 1183–1186.
- Stewart-Ornstein J, Weissman JS, El-Samad H (2012) Cellular noise regulons underlie fluctuations in *Saccharomyces cerevisiae*. *Mol Cell* 45: 483–493.
- Typas A, Becker G, Hengge R (2007) The molecular basis of selective promoter activation by the σ^S subunit of RNA polymerase. *Mol Microbiol* 63: 1296–1306.
- Chiang SM, Schellhorn HE (2010) Evolution of the RpoS regulon: origin of RpoS and the conservation of RpoS-dependent regulation in bacteria. *J Mol Evol* 70: 557–571.
- Ilves H, Horak R, Kivisaar M (2001) Involvement of σ^S in starvation-induced transposition of *Pseudomonas putida* transposon Tn4652. *J Bacteriol* 183: 5445–5448.
- Perez-Osorio AC, Williamson KS, Franklin MJ (2010) Heterogeneous *rpoS* and *rhlR* mRNA levels and 16S rRNA/rDNA (rRNA gene) ratios within *Pseudomonas aeruginosa* biofilms, sampled by laser capture microdissection. *J Bacteriol* 192: 2991–3000.
- Locke JC, Young JW, Fontes M, Hernandez Jimenez MJ, Elowitz MB (2011) Stochastic pulse regulation in bacterial stress response. *Science* 334: 366–369.
- Eldar A, Elowitz MB (2010) Functional roles for noise in genetic circuits. *Nature* 467: 167–173.
- Ito Y, Toyota H, Kaneko K, Yomo T (2009) How selection affects phenotypic fluctuation. *Mol Syst Biol* 5: 264.
- Ditta G, Stanfield S, Corbin D, Helinski DR (1980) Broad host range DNA cloning system for gram-negative bacteria: construction of a gene bank of *Rhizobium meliloti*. *Proc Natl Acad Sci U S A* 77: 7347–7351.
- Stolz A, Busse HJ, Kampfer P (2007) *Pseudomonas knackmussii* sp. nov. *Int J Syst Evol Microbiol* 57: 572–576.

Acknowledgments

The authors thank Kamila Czechowska and Bebek Gjoksi for their assistance in preliminary experiments.

Author Contributions

Conceived and designed the experiments: JRvdM MM RM FR. Performed the experiments: RM MM SS NP. Analyzed the data: JRvdM RM NP FR SS. Contributed reagents/materials/analysis tools: RM MM NP FR SS. Wrote the paper: JRvdM RM MM NP.

50. Ravatn R, Zehnder AJ, van der Meer JR (1998) Low-frequency horizontal transfer of an element containing the chlorocatechol degradation genes from *Pseudomonas* sp. strain B13 to *Pseudomonas putida* F1 and to indigenous bacteria in laboratory-scale activated-sludge microcosms. *Appl Environ Microbiol* 64: 2126–2132.
51. Sambrook J RD (2001) *Molecular cloning: a laboratory manual*, third edn. Cold Spring Harbor: Cold Spring Harbor Laboratory Press.
52. Gerhardt P MR, Costilow RN, Nester EW, Wood WA, Krieg NR, et al. (1981) *Manual of methods for general bacteriology*. American Society for Microbiology.
53. Gaillard M, Pernet N, Vogne C, Hagenbuchle O, van der Meer JR (2008) Host and invader impact of transfer of the *clc* genomic island into *Pseudomonas aeruginosa* PAO1. *Proc Natl Acad Sci U S A* 105: 7058–7063.
54. Altschul SF, Lipman DJ (1990) Protein database searches for multiple alignments. *Proc Natl Acad Sci U S A* 87: 5509–5513.
55. Laville J, Voisard C, Keel C, Maurhofer M, Defago G, et al. (1992) Global control in *Pseudomonas fluorescens* mediating antibiotic synthesis and suppression of black root rot of tobacco. *Proc Natl Acad Sci U S A* 89: 1562–1566.
56. Kristensen CS, Eberl L, Sanchez-Romero JM, Givskov M, Molin S, et al. (1995) Site-specific deletions of chromosomally located DNA segments with the multimer resolution system of broad-host-range plasmid RP4. *J Bacteriol* 177: 52–58.
57. Martinez-Garcia E, Calles B, Arevalo-Rodriguez M, de Lorenzo V (2011) pBAM1: an all-synthetic genetic tool for analysis and construction of complex bacterial phenotypes. *BMC Microbiol* 11: 38.
58. Sentschilo VS, Zehnder AJB, van der Meer JR (2003) Characterization of two alternative promoters and a transcription regulator for integrase expression in the *clc* catabolic genomic island of *Pseudomonas* sp. strain B13. *Mol Microbiol* 49: 93–104.
59. Kristensen CS, Eberl L, Sanchez-Romero JM, Givskov M, Molin S, et al. (1995) Site-specific deletions of chromosomally located DNA segments with the multimer resolution system of broad-host-range plasmid RP4. *J Bacteriol* 177: 52–58.
60. Martinez-Garcia E, de Lorenzo V (2011) Engineering multiple genomic deletions in Gram-negative bacteria: analysis of the multi-resistant antibiotic profile of *Pseudomonas putida* KT2440. *Environ Microbiol* 13: 2702–2716.
61. McClure NC, Weightman AJ, Fry JC (1989) Survival of *Pseudomonas putida* UWC1 containing cloned catabolic genes in a model activated-sludge unit. *Appl Environ Microbiol* 55: 2627–2634.